

Three-nucleon correlations in light nuclei yield ratios from the AMPT model for QCD critical point investigations*

Ning Yu (喻宁)^{1,2†} Zuman Zhang (张祖满)^{1,2} Hongge Xu (徐鸿鸽)^{1,2} Zhong Zhu (朱仲)^{1,3}

¹School of Physics and Mechanical Electrical and Engineering, Hubei University of Education, Wuhan 430205, China

²Institute of Theoretical Physics, Hubei University of Education, Wuhan 430205, China

³Institute of Quantum Matter, South China Normal University, Guangzhou 510631, China

Abstract: This study uses the AMPT model in Au+Au collisions to study the influence of the three nucleon correlation C_{n^2p} on light nuclei yield ratios. Neglecting C_{n^2p} results in an overestimated relative neutron density fluctuation extraction. In contrast, including C_{n^2p} enhances the agreement with experimental results with higher yield ratios but does not change the energy dependence of the yield ratio. Since the AMPT model does exhibit a first-order phase transition or critical physics, the study fails to reproduce the experimental energy-dependent peak around $\sqrt{s_{NN}}=20-30$ GeV. The study's findings might offer a baseline for investigating critical physics phenomena using light nuclei production as a probe.

Keywords: QCD Critical Point, light nuclei yield ratios, AMPT, three-nucleon correlation

DOI: 10.1088/1674-1137/ad9306 **CSTR:** 32044.14.ChinesePhysicsC.49054101

I. INTRODUCTION

Quantum chromodynamics (QCD), the bedrock theory of strong interactions between quarks and gluons, has motivated the exploration of QCD phase diagrams [1] to map the behavior of QCD matter under extreme conditions. One of the pivotal objectives of the Beam Energy Scan (BES) program at the Relativistic Heavy-Ion Collider (RHIC) is the search for the elusive QCD critical point [2–7]. This research is also a key motivation for future accelerators, such as the Facility for Anti-Proton and Ion Research (FAIR) in Darmstadt and the Nuclotron-based Ion Collider fAcility (NICA) in Dubna.

Close to the QCD critical point, fluctuations in conserved quantities, notably baryon number (B), charge (Q), and strangeness (S), are expected [8]. The production of light nuclei is predicted to be sensitive to baryon density fluctuations under the premise that the nuclei are formed by the coalescence of nucleons [9, 10]. The light nuclei yield ratio, expressed as $N_p N_t / N_d^2$, which encompasses the production of proton (p), deuteron (d), and triton (t), can be posited to be delineated by the relative neutron density fluctuation ($\Delta\rho_n$) and the correlation between neutron and proton densities at the kinetic freeze-out point. Notably, the STAR collaboration has reported a non-monotonic energy dependence of the yield ratio that peaks around 20–30 GeV in the most central Au+Au collisions [11, 12].

If correlations between neutron and proton densities are disregarded, the light nuclei yield ratio has direct proportionality with relative neutron density fluctuations. Experimental observations have implied the existence of a large relative neutron density fluctuation at this energy range.

In our previous work [13], we used the AMPT model to investigate the impact of the two-body neutron-proton density correlation, C_{np} , on the yield ratio of light nuclei. We arrived at the conclusion that the correlation C_{np} has a slight effect on the light nuclei yield ratio at central or mid-central Au+Au collisions. In other words, experimentalists can extract the relative neutron density fluctuation directly from the light nuclei yield ratio. In contrast, for peripheral collisions, the effect of C_{np} on the light nuclei yield ratio increases and related effects must be considered when extracting the density fluctuation. However, a critical aspect overlooked in that study concerned the three-nucleon correlation involving two neutrons and one proton, C_{n^2p} , which directly influences triton yields and, consequently, the overall light nuclei yield ratio. Because tritons are products of coalescence processes involving multiple nucleons, the inclusion of C_{n^2p} is pivotal for a comprehensive understanding of light nuclei formation dynamics and the accurate extraction of relative neutron density fluctuations from experimental data.

Therefore, this study aims to build on our previous findings by delving into the influence of the three-nucle-

Received 7 July 2024; Accepted 13 November 2024; Published online 14 November 2024

* Supported in part by the Scientific Research Foundation of Hubei University of Education for Talent Introduction (ESRC20230002, ESRC20230007) and Research Project of Hubei Provincial Department of Education (D20233003, B2023191)

† E-mail: ning.yuchina@gmail.com

©2025 Chinese Physical Society and the Institute of High Energy Physics of the Chinese Academy of Sciences and the Institute of Modern Physics of the Chinese Academy of Sciences and IOP Publishing Ltd. All rights, including for text and data mining, AI training, and similar technologies, are reserved.

on correlation C_{n^2p} on the light nuclei yield ratio. Through this enhanced analysis, we expect to show the importance of C_{n^2p} on the extraction of relative neutron density fluctuations from the light nuclei yield ratio, thereby offering insights for the quest of identifying the QCD critical point. This paper is structured as follows: we commence with a review of the AMPT model. We then show the definition of the three-nucleon correlation and its connection to the light nuclei yield ratio. Subsequently, we present our results on the dependence of the three-nucleon correlation on rapidity coverage, collision centrality, and energy. Finally, we discuss the implications of the C_{n^2p} on the light nuclei yield ratio and its observed energy-dependent behavior in experiments.

II. MODEL

AMPT, a multi-phase transport model, is a hybrid model consisting of four components: initial conditions, partonic interactions, partonic matter to hadronic matter conversion, and hadronic interactions [14]. The default version of the AMPT model involves only mini-jet partons in its parton cascade and uses the Lund string fragmentation for parton hadronization [15]. Conversely, the string melting version of the AMPT model involves the conversion of all excited strings into partons and the use of a quark coalescence model to describe parton hadronization. Typically, the default version gives a reasonable description of $dN/d\eta$, dN/dy , and the p_T spectra, while the string melting version describes the magnitude of the elliptic flow but not the p_T spectra. The string melting version, with a modified set of parameters, can well reproduce the p_T spectra and elliptic flows at the RHIC top energy [16]. In this paper, all the results are studied using this set of parameters.

Based on Refs. [9, 11] and our preceding work [13], we commence with a review of the nucleon coalescence model and its consequent estimations of light nuclear yields. Ignoring the binding energy of light nuclei, their abundance can be formulated as follows:

$$N_c = g_c A^{3/2} \left(\frac{2\pi}{m_0 T_{\text{eff}}} \right)^{3(A-1)/2} V \langle \rho_p \rangle^{A_p} \langle \rho_n \rangle^{A_n} \sum_{i=0}^{A_p} \sum_{j=0}^{A_n} C_{A_p}^i C_{A_n}^j C_{n^j p^i}. \quad (1)$$

Here, $g_c = \frac{2S+1}{2^A}$ represents the coalescence factor for $A = A_n + A_p$ nucleons of spin 1/2 forming a cluster with a total spin of S . The same nucleon mass m_0 is considered for both protons and neutrons. V denotes the system volume, and T_{eff} is the effective temperature at kinetic freeze-out. $\langle \rho_n \rangle$ and $\langle \rho_p \rangle$ are the neutron and proton density. Combinations are represented by $C_{A_p}^i$ and $C_{A_n}^j$. $C_{n^j p^i}$ is the correlation between j -neutrons and i -protons,

defined as:

$$C_{n^j p^i} = \frac{\langle \delta \rho_p^i \delta \rho_n^j \rangle}{\langle \rho_p \rangle^i \langle \rho_n \rangle^j}. \quad (2)$$

The relative neutron density fluctuation $\Delta \rho_n = \sigma_n^2 / \langle \rho_n \rangle^2$ is equivalent to $C_{n^2 p^0}$. The two-body neutron-proton density correlation, C_{np} , is given by:

$$C_{np} = \frac{\langle \delta \rho_p \delta \rho_n \rangle}{\langle \rho_p \rangle \langle \rho_n \rangle} = \frac{\langle \rho_p \rho_n \rangle}{\langle \rho_p \rangle \langle \rho_n \rangle} - 1. \quad (3)$$

The three-nucleon correlation, $C_{n^2 p}$, can be expressed as

$$C_{n^2 p} = \frac{\langle \delta \rho_p \delta \rho_n^2 \rangle}{\langle \rho_p \rangle \langle \rho_n \rangle^2} = \frac{\langle \rho_p \rho_n^2 \rangle}{\langle \rho_p \rangle \langle \rho_n \rangle^2} - (1 + 2C_{np}). \quad (4)$$

Employing these formulations, the yields of deuteron and triton are specified as:

$$N_d = \frac{3}{2^{1/2}} \left(\frac{2\pi}{m_0 T_{\text{eff}}} \right)^{3/2} V \langle \rho_p \rangle \langle \rho_n \rangle (1 + C_{np}), \quad (5)$$

$$N_t = \frac{3^{3/2}}{4} \left(\frac{2\pi}{m_0 T_{\text{eff}}} \right)^3 V \langle \rho_p \rangle \langle \rho_n \rangle^2 (1 + \Delta \rho_n + 2C_{np} + C_{n^2 p}). \quad (6)$$

Subsequently, the light nuclei yield ratio is compactly presented as:

$$R = \frac{1}{2\sqrt{3}} \frac{1 + \Delta \rho_n + 2C_{np} + C_{n^2 p}}{(1 + C_{np})^2}. \quad (7)$$

The three-nucleon correlation $C_{n^2 p}$ exerts a significant influence on the light nuclei yield ratios, effectively enhancing them. Assuming the three-nucleon correlation $C_{n^2 p}$ is zero, Eq. (7) simplifies to:

$$R = \frac{1}{2\sqrt{3}} \frac{1 + \Delta \rho_n + 2C_{np}}{(1 + C_{np})^2}. \quad (8)$$

Taking the analysis a step further, if the two-nucleon correlation C_{np} is also neglected, the light nuclei yield ratio is further simplified and can be expressed as:

$$R = \frac{1 + \Delta \rho_n}{2\sqrt{3}}. \quad (9)$$

In this highly simplified scenario, the yield ratio is directly proportional to the relative neutron density fluctuation $\Delta \rho_n$, which forms the experimental basis for extracting the $\Delta \rho_n$ from the yield ratios of light nuclei.

Following the procedure in our preceding work, the event-by-event multiplicity and fluctuation of the proton $\langle N_p \rangle$, S_p , neutron $\langle N_n \rangle$, S_n and their mixed moments $\langle N_p N_n \rangle$, $\langle N_p N_n^2 \rangle$ can be extracted from the AMPT model. When calculating $\Delta\rho_p, \Delta\rho_n$, the system volume effects are eliminated. In the AMPT model, nucleon production is analyzed across varying rapidity intervals and collision centralities. The definition of centrality is determined by the per-event charged particle multiplicity N_{ch} for the pseudorapidity range $\eta \leq 0.5$.

III. RESULTS AND DISCUSSION

Figure 1 illustrates the rapidity coverage dependence of the dimensionless statistics $\sigma_n/\langle n \rangle$, $\sigma_p/\langle p \rangle$, C_{np} , C_{n^2p} , and C_{np^2} for 0–10% Au+Au collisions at $\sqrt{s_{NN}} = 200$ GeV. $\sigma_p/\langle \rho_p \rangle$ and $\sigma_n/\langle \rho_n \rangle$, which can be regarded as relative nucleon density fluctuations, decrease with increasing rapidity coverage. It can be found that the relative density fluctuation for neutrons $\sigma_n/\langle n \rangle$ and protons $\sigma_p/\langle p \rangle$ are roughly equivalent and decrease with increasing rapidity coverage. In the smaller rapidity coverage region, especially at mid-rapidity, particle pair production dominates. Consequently, nucleon density fluctuations are relatively larger at mid-rapidity compared to a wider rapidity coverage. The correlation C_{np} is independent of rapidity coverage and almost vanishes for 0–10% Au+Au collisions at $\sqrt{s_{NN}} = 200$ GeV. Similar results are

observed between the correlation C_{n^2p} for two neutrons and one proton and the correlation C_{np^2} for one neutron and two protons. The behavior of C_{n^2p} is similar to that of the relative neutron density fluctuations $\sigma_n/\langle n \rangle$, with both decreasing with increasing rapidity coverage.

The lower panel in Fig. 1 presents the light nuclei yield ratios calculated using Eqs. (7), (8), and (9), demonstrating the comprehensive influence of both C_{np} and C_{n^2p} , the effects of C_{np} without C_{n^2p} , and the scenario without any nucleon correlation effects C_{np} and C_{n^2p} . We also draw the line of $1/2\sqrt{3}$, which holds for scenarios without both relative neutron density fluctuation and nucleon correlations. It is observed that, due to the near-zero value of C_{np} for central collisions, its impact on the light nuclei yield ratios is insignificant. Moreover, since C_{n^2p} exhibits a similar dependence on the rapidity coverage as the relative neutron density fluctuation $\sigma_n/\langle n \rangle$, including C_{n^2p} increases the calculated light nuclei yield ratios. Consequently, if C_{n^2p} is disregarded in the analysis, employing Eq. (8) to extract the relative neutron density fluctuation from the light nuclei yield ratios would yield an overestimated value compared compared to actual physical figure.

The top panel of Fig. 2 shows the rapidity coverage dependence of $\sigma_n/\langle n \rangle$, $\sigma_p/\langle p \rangle$, C_{np} , C_{n^2p} , and C_{np^2} for 60%–80% Au+Au collisions at $\sqrt{s_{NN}} = 39$ GeV. Consistent with the findings from central collisions, $\sigma_p/\langle \rho_p \rangle$, $\sigma_n/\langle \rho_n \rangle$, and C_{np^2} decrease with increasing rapidity cover-

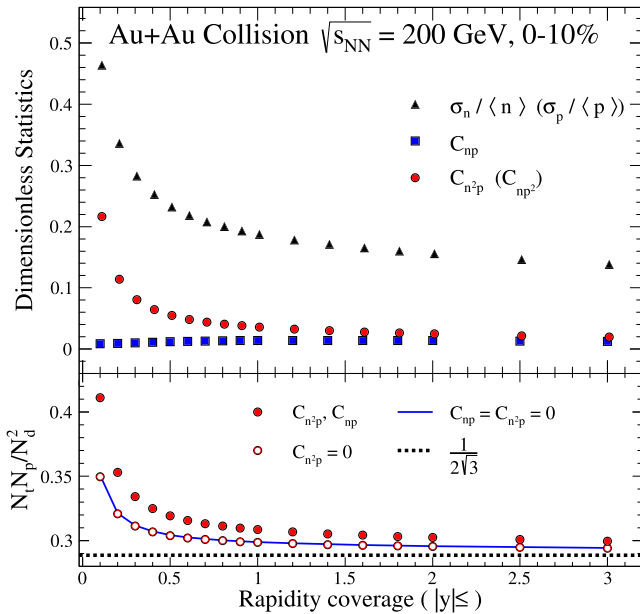


Fig. 1. (color online) Top panel: Dimensionless statistics $\sigma_n/\langle n \rangle$, $\sigma_p/\langle p \rangle$, C_{np} , C_{n^2p} , and C_{np^2} for 0–10% Au+Au collisions at $\sqrt{s_{NN}} = 200$ GeV. Bottom panel: The light nuclei yield ratio $N_t N_p / N_d^2$ calculated from the top panel shown as solid circles for Eq. (7), opened circles for Eq. (8), and a solid line for Eq. (9).

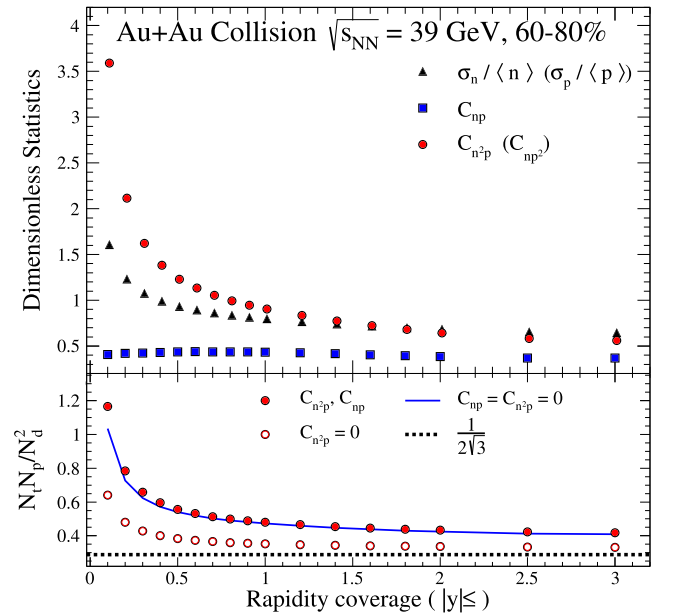


Fig. 2. (color online) Top panel: Dimensionless statistics $\sigma_n/\langle n \rangle$, $\sigma_p/\langle p \rangle$, C_{np} , C_{n^2p} , and C_{np^2} for 60%–80% Au+Au collisions at $\sqrt{s_{NN}} = 39$ GeV. Bottom panel: The light nuclei yield ratio $N_t N_p / N_d^2$ calculated from the top panel are shown as solid circles for Eq. (7), open circles for Eq. (8), and solid lines for Eq. (9).

age. At a given rapidity coverage, these quantities are greater in peripheral collisions compared to those in central collisions. For instance, the convergence value of $\sigma_p/\langle\rho_p\rangle$ at larger rapidity coverages is approximately 0.7 for peripheral collisions, whereas it is roughly 0.14 for central collisions at $\sqrt{s_{NN}} = 39$ GeV. C_{np} is independent of rapidity coverage for a non-negligible value of 0.45 – 0.5 in peripheral collisions. Consequently, the influence of both C_{np} and C_{n^2p} on the related light nuclei yield ratio in peripheral collisions is evident in the bottom panel of Fig. 2. Specifically, the exclusion of C_{n^2p} yields a reduced light nuclei yield ratio, that is, a change from the solid circles to the open circles. Conversely, when C_{np} is not considered, the light nuclei yield ratio is increases, reflected by the shift from the open circles to the solid line. The impact of C_{np} and C_{n^2p} on the light nuclei yield ratio are contrasting. When both are considered, the deviation in the yield ratio from that obtained by neglecting both depends critically on the magnitude of their respective effects. Notably, the figure illustrates that for 60% – 80% Au+Au collisions at $\sqrt{s_{NN}} = 39$ GeV, the effects of these two factors nearly offset each other. In other words, in this particular case, considering both C_{np} and C_{n^2p} yields results similar to those derived when neither is considered. This highlights that, at least in this instance, the net effect of incorporating C_{np} and C_{n^2p} in the analysis does not significantly change the light nuclei yield ratio.

The top panel of Fig. 3 illustrates the centrality de-

pendence of $\sigma_n/\langle n\rangle$, $\sigma_p/\langle p\rangle$, C_{np} , C_{n^2p} , and C_{np^2} for Au+Au collisions at $\sqrt{s_{NN}} = 19.6$ GeV, confined to a rapidity coverage of $|y| \leq 0.5$. Notably, these quantities increase as the collisions transition from central to peripheral collisions. The corresponding light nuclei yield ratio calculated using Eqs. (7), (8), and (9) are presented at the bottom of Fig. (3). These illustrate the influence of C_{np} and C_{n^2p} on these yields. At central or mid-central collision, the variation between the yield ratios given by Eqs. (8) and (9) is very small, implying that the influence of C_{np} on the yield ratios can effectively be disregarded in these collisions. Conversely, in peripheral collisions, the effect of C_{np} on the yield ratios becomes significant and cannot be ignored. Furthermore, it is observed that C_{n^2p} exerts a positive effect on the yield ratios, increasing the light nuclei yield ratio. In contrast, C_{np} exerts a negative effect on the yield ratios. Consequently, when both C_{np} and C_{n^2p} are considered, in central and mid-central collisions, C_{n^2p} is dominant, leading to an increase in the yield ratio. However, in peripheral collisions, the influences of these two factors may offset each other.

Centrality bin width correction is important for any event-by-event fluctuation calculation. In Fig. 4, we present the light nuclei yield ratios obtained from different centrality bin widths centered around six centrality. The x-axis represents the centrality bin width. For example, for the red solid triangles, a centrality width of 2% corresponds to collisions within the centrality of 6% – 7%, while a centrality width of 5% corresponds to collisions within the centrality of 0 – 10%, representing the central collisions reported in this study. Similarly, for the opened

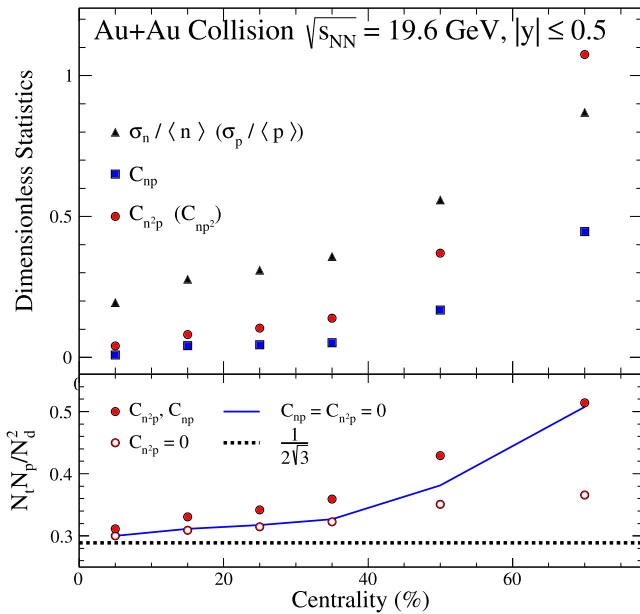


Fig. 3. (color online) Top panel: Dimensionless statistics $\sigma_n/\langle n\rangle$, $\sigma_p/\langle p\rangle$, C_{np} , C_{n^2p} , and C_{np^2} for Au+Au collisions at $\sqrt{s_{NN}} = 19.6$ GeV with $|y| \leq 0.5$. Bottom panel: The light nuclei yield ratio $N_t N_p / N_d^2$ calculated from the top panel are shown as solid circles for Eq. (7), open circles for Eq. (8), and solid line for Eq. (9).

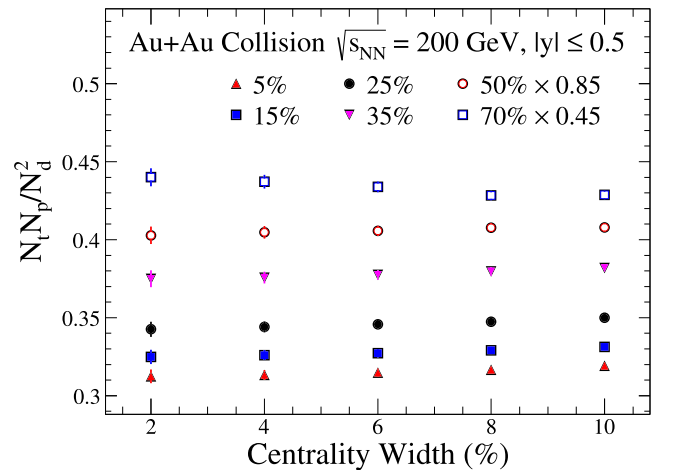


Fig. 4. (color online) Centrality bin width dependence of the light nuclei yield ratio $N_t N_p / N_d^2$ from the AMPT model for Au+Au collisions at $\sqrt{s_{NN}} = 200$ GeV with $|y| \leq 0.5$. The different symbols represent results obtained at different centrality centered around specific centrality values (5%, 15%, 25%, 35%, 50%, 70%). Data points for centrality centers of 50% and 70% are scaled by factors of 0.85 and 0.45, respectively, for clarity.

circles, a centrality width of 6% indicates the centrality of 47% – 53%. To better illustrate the results, the data points corresponding to centrality centers of 50% and 70% are multiplied by factors of 0.85 and 0.45, respectively. As shown in the figure, except for the most peripheral collisions, for a given centrality center value, the light nuclei yield ratios increase slightly with increasing centrality width, with the increase being approximately between 2% and 4%. This suggests that the influence of the centrality bin width on the light nuclei yield ratios is relatively minor.

Figure 5 illustrates the collision energy dependence of the light nuclei yield ratio $N_t N_p / N_d^2$ extracted from 0 – 10% central and 60% – 80% peripheral Au+Au collisions within $|y| \leq 0.5$. The dash-dot lines represent cases where C_{np} and C_{n^2p} are disregarded. A slight increase in the light nuclei yield ratio with increasing collision energy is evident from the AMPT model. At 0 – 10% central collisions, the yield ratios are consistent with predictions from the coalescence model calculations, $1/2\sqrt{3}$. Peripheral collisions show larger yield ratios in comparison to central collisions. When C_{n^2p} is not considered, the yield ratio for both central and peripheral collisions is reduced, suggesting that neglecting C_{n^2p} would yield an overestimate of neutron density fluctuations from experimental data. Interestingly, the discrepancy between experimental and actual physical signals, induced by the omission of C_{n^2p} , remains unaffected by the collision energy, except at lower energies, specifically at 7.7 GeV. At a lower energy regime, the influence of C_{n^2p} on the yield ratio becomes more important, whose underlying mechanisms are unclear and constitute a focal point for future research.

Figure 6 compares the experimental results from STAR at 0 – 10% central Au+Au collisions [12] and NA49 at central Pb+Pb collisions [9, 17]. Since we compare the central collisions, the impact of C_{np} on the yield from the AMPT model is deemed negligible. The inclusion of C_{n^2p} enhances the light nuclei yield ratios, bringing the AMPT model estimates closer to the experimental results. However, the inclusion of C_{n^2p} does not change the collision energy dependence of the yield ratio, thereby failing to reproduce the non-monotonic behavior observed in experiments. Given the absence of critical phenomena in the AMPT, this result is reasonable. Using the AMPT model, we obtain a better baseline of the light nuclei yield ratio.

IV. SUMMARY

In summary, using the AMPT model for Au+Au collisions, we study the rapidity, collision energy, and centrality dependence of the relative neutron density fluctuation $\sigma_n / \langle n \rangle$ and the two nucleons and three nucleons correlations C_{np} and C_{n^2p} . The related light nuclei yield ra-

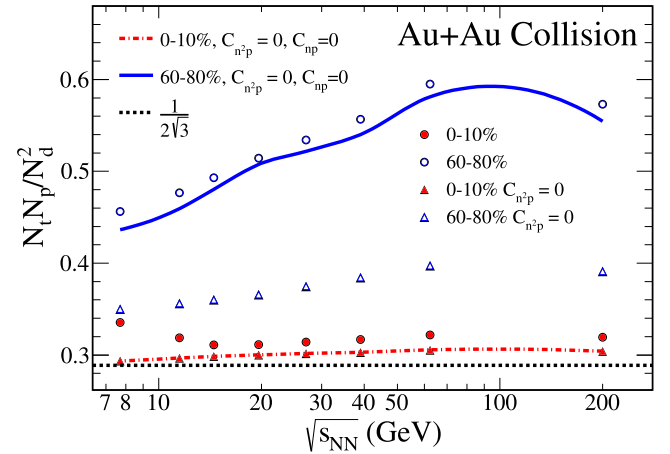


Fig. 5. (color online) Collision energy dependence of the light nuclei yield ratio $N_t N_p / N_d^2$ from the AMPT model for Au+Au collisions with $|y| \leq 0.5$. The results from 0 - 10% central Au+Au collision are shown as solid circles for Eq. (7), solid triangles for Eq. (8) and a red dashed line for Eq. (9). The results from 60% - 80% peripheral Au+Au collision are shown as open circles for Eq. (7), open triangles for Eq. (8), and a blue dashed line for Eq. (9).

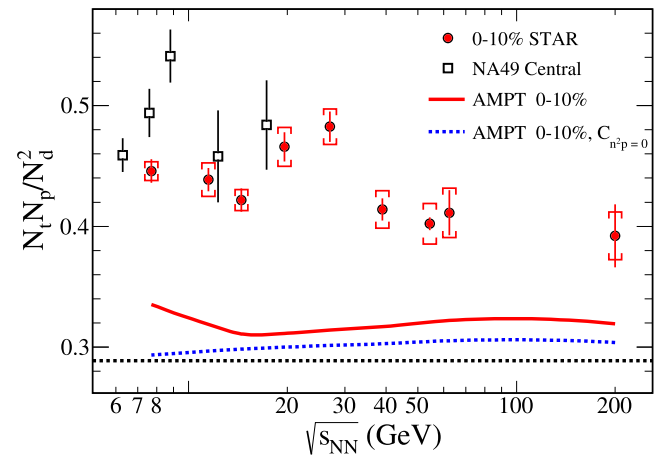


Fig. 6. (color online) Collision energy and centrality dependence of the light nuclei yield ratio $N_t N_p / N_d^2$ from the AMPT model with $|y| \leq 0.5$. Solid circles are the results from the STAR detector at 0 – 10% central Au+Au collision [12]. Open squares are the results from NA49 at central Pb+Pb collision [9, 17].

tios obtained using Eqs. (7), (8), and (9) are also investigated. At central or mid-central collisions, the influence of C_{np} on the light nuclei yield ratios is insignificant. However, in peripheral collisions, a non-zero C_{np} reduces the light nuclei yield ratio. Importantly, regardless of central or peripheral collisions, the C_{n^2p} leads to an overall enhancement in the light nuclei yield ratios. Owing to the absence of critical physics in the AMPT model, it fails to reproduce the experimental observations, particularly the peak observed in the light nuclei yield ratio

around $\sqrt{s_{NN}} = 20 - 30$ GeV. Incorporating the three-nucleon correlation C_{n^2p} , our model produces results that offer a more accurate baseline that is closer to the true experimental values.

ACKNOWLEDGEMENTS

The authors appreciate the referee for his/her careful reading of the paper and valuable comments.

References

- [1] P. Braun-Munzinger and J. Wambach, *Rev. Mod. Phys.* **81**, 1031 (2009)
- [2] Z. Fodor, S. D. Katz, and K. K. Szabó, *Phys. Lett. B* **568**, 73 (2003)
- [3] Z. Fodor and S. D. Katz, *J. High Energy Phys.* **2004**, 050 (2004)
- [4] R. V. Gavai and S. Gupta, *Phys. Rev. D* **71**, 114014 (2005)
- [5] F. Karsch *et al.*, *Nucl. Phys. A* **956**, 352 (2016)
- [6] S. Gupta, X. Luo, B. Mohanty *et al.*, *Science* **332**, 1525 (2011)
- [7] M. Stephanov, PoS LAT **2006**, 024 (2006)
- [8] M. Stephanov, K. Rajagopal, and E. Shuryak, *Phys. Rev. D* **60**, 114028 (1999)
- [9] K.-J. Sun, L.-W. Chen, C. M. Ko *et al.*, *Phys. Lett. B* **781**, 499 (2018)
- [10] N. Yu, D. Zhang, and X. Luo, *Chin. Phys. C* **44**, 014002 (2020)
- [11] H. Liu, D. Zhang, S. He *et al.*, *Phys. Lett. B* **805**, 135452 (2020)
- [12] M. I. Abdulhamid *et al.* (STAR Collaboration), *Phys. Rev. Lett.* **130**, 202301 (2023)
- [13] Z. Zhang, N. Yu, and H. Xu, *Eur. Phys. J. A* **58**, 240 (2022)
- [14] Z.-W. Lin, C. M. Ko, B.-A. Li *et al.*, *Phys. Rev. C* **72**, 064901 (2005)
- [15] B. Andersson, G. Gustafson, G. Ingelman *et al.*, *Phys. Rep.* **97**, 31 (1983)
- [16] Z.-W. Lin, *Phys. Rev. C* **90**, 014904 (2014)
- [17] T. Anticic *et al.*, *Phys. Rev. C* **94**, 044906 (2016)